

Observation of Spin Flip in $^{13}\text{C} + ^{24}\text{Mg}$ Inelastic Scattering

W. Dünneweber,^(a) P. D. Bond, C. Chasman, and S. Kubono^(b)

Brookhaven National Laboratory, Upton, New York 11973

(Received 17 September 1979)

Evidence for spin-dependent interactions in heavy-ion reactions has been found in the inelastic scattering of 35-MeV ^{13}C from the 1.368-MeV, 2^+ state in ^{24}Mg . γ rays emitted perpendicular to the reaction plane have been measured and $|m|$ -substate populations deduced. At ^{13}C scattering angles $\theta_{\text{c.m.}} = 10^\circ$ and 21° , probabilities for the $|m| = 1$ population (which is equivalent to spin flip) are found to be $(1.7 \pm 0.5)\%$ and less than 0.8% , respectively.

Little is known about spin-dependent interactions, and specifically the spin-orbit interaction, between heavy ions. The values of the real spin-orbit potential calculated by several authors¹⁻³ within the folding-model framework vary by an order of magnitude but do not exceed 0.5% of the spin-independent real potential in the nuclear surface region for ^{13}C or ^{19}F incident upon medium-weight nuclei at few MeV per nucleon. On the other hand, much stronger spin-orbit potentials have been put forward⁴⁻⁶ in order to fit, within the framework of the distorted-wave Born approximation (DWBA), the measured differential cross sections of transfer reactions involving ^{19}F , ^{13}C , or ^{15}N .

In this Letter we report direct evidence for a spin-dependent interaction in the inelastic scattering of ^{13}C by ^{24}Mg , obtained by detection of spin flip. The method, detection of γ rays emitted perpendicular to the reaction plane, has been established⁷ in light-ion physics as an alternative to studies of the analyzing power in polarized-ion scattering [the heaviest ion for which the latter method has been applied is ^6Li (Ref. 8)]. As was shown by Bohr,⁹ in a two-body reaction leading to pure parity states, symmetry about the reaction plane restricts the allowed combinations of the initial and final nuclear spin projections along the scattering normal (which we choose as quantization axis). In the case of the reaction $^{24}\text{Mg}(^{13}\text{C}, ^{13}\text{C}')^{24}\text{Mg}(2^+)$ with ^{13}C ($^{13}\text{C}'$) spin projections $m_{1/2}$ ($m_{1/2}'$), Bohr's theorem reads

$$\exp\{i\pi(m_{1/2} - m_{1/2}')\} = \exp\{i\pi m\},$$

where m is the spin projection of the 2^+ state of ^{24}Mg . Thus, even values of m correspond to the spin-nonflip processes and $|m| = 1$ to spin-flip processes in the projectile.

Since the 2^+ state decays to the 0^+ ground state, the radiative transition must have $|\Delta m| = |m|$. At $\theta_\gamma = 0^\circ$ (the direction of the scattering normal) only the $|m| = 1$ component has a nonvanishing

γ -ray intensity; so a measurement at that angle is a sensitive measure of the spin-flip probability. However, the finite solid angle of the γ detector also allows contributions from the other $|m|$ components. The probabilities P_m of the $|m|$ components, normalized by $P_0 + P_1 + P_2 = 1$, may be determined by two measurements with a cylindrical γ detector positioned along the quantization axis at two different distances from the target. The basis of this simple procedure is that (a) the detector symmetry results in integration over the azimuthal angle leaving the correlation dependent only upon the population parameters, P_m , and (b) the radiation patterns for the $|m|$ components differ strongly so the relative detection efficiency changes rapidly with the detector distance to the target.

Isotopically enriched ^{24}Mg targets of 40 to 70 $\mu\text{g}/\text{cm}^2$ thickness evaporated on thin ^{12}C backings were bombarded with a 35-MeV ^{13}C beam from the Brookhaven National Laboratory tandem Van de Graaff facility. A 9-cm² Si-detector was used to detect the $^{13}\text{C}^{6+}$ inelastic-scattering products in the focal plane of the Brookhaven quadrupole-triple-dipole magnetic spectrometer. This detector also provided the particle time signal for the coincidence circuit. After each run a large-area position-sensitive ΔE - E proportional counter was moved into the same position in the focal plane to ensure the unambiguous identification of the inelastic $^{13}\text{C}^{6+}$ and to determine the ^{13}C elastic background under the $^{24}\text{Mg}(2^+)$ peak. Guided by the DWBA prediction of a steep, oscillatory increase of the spin-flip cross section towards forward angles, rather small scattering angles, $\theta_{\text{c.m.}} = 10^\circ$ and 21° ($\theta_{\text{lab}} = 6.3^\circ$ and 13.4°), were chosen for the coincidence measurements. The scattering normal was defined within $\pm 2.5^\circ$ at these angles by using narrow vertical-slit openings of ± 1.5 and ± 3 mm, respectively, at the entrance of the magnetic spectrograph. The horizontal slit openings were set to $\pm 1.1^\circ$.

The coincident γ radiation was detected with a 3-in. \times 3-in. NaI detector (covered with a 0.8-mm-thick lead and a 0.1-mm-thick copper absorber) positioned in the direction of the scattering normal at various distances, d , from the target (Table I). The experiment was divided into several runs at alternating distances with results at each distance consistent within the statistical errors. Figure 1 shows the γ -ray spectrum, summed over five separate runs, for $d = 14.6$ cm before subtraction of random coincidences (about 5% of the 1.37-MeV photopeak yield). Calculated^{10,11} photopeak efficiencies $\eta(d)$ for isotropic radiation agreed to within 5% with *in situ* measurements with calibrated sources.

The results of our measurements are listed in Table I in terms of the γ yield per particle event, $I_\gamma(d)$, obtained by dividing the number of coincident photopeak counts (see Fig. 1) by the particle singles yield, which was recorded simultaneously. Note that the cross section and effective solid angle for the particles cancel in this ratio. For the $\theta_{c.m.} = 10^\circ$ measurements the values of I_γ/η are displayed in Fig. 2. The effect of the radiation patterns on the detection efficiency for each $|m|$ is also demonstrated; the dashed curves give the calculated¹¹ photopeak efficiency $\eta_m(d)$ normalized by $\eta(d)$ for the $|m|=0, 1, 2$ components of the E_2 , 1.368-MeV radiative transition. By comparison, the measured values show the dominance of the $|m|=2$ component but also the presence of a small $|m|=1$ component which becomes evident at large d . The measurements, performed at three distances, correspond to a set of three equations for two unknown parameters which have

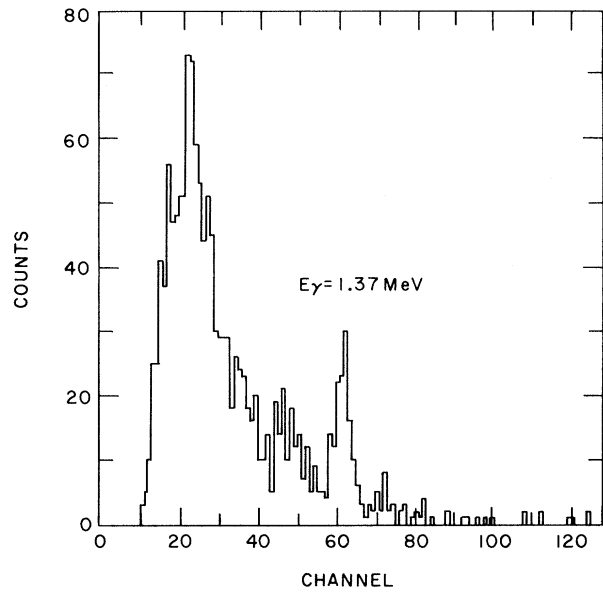


FIG. 1. γ -ray coincidence spectrum at $d = 14.6$ cm for a ^{13}C scattering angle of 10° c.m. About 40% of the counts in the $E_\gamma = 1.37$ -MeV peak originate from spin-flip events.

been chosen as P_1 and P_2 :

$$I_\gamma(d) = \eta_0(d)(1 - P_1 - P_2) + \eta_1(d)P_1 + \eta_2(d)P_2.$$

A least-squares fit yields the P_m values given in Table I. The I_γ/η curve resulting from the fit is shown in Fig. 2. We find an $|m|=1$ component of 1.7% at the more forward angle. At 21° the fit yields P_0 and P_1 values consistent with zero. The additional constraint $P_0 \geq 0$ results in $P_1 < 0.3\%$. The $|m|=2$ component constitutes about 90% of the cross section at both angles. As indicated by the different statistical errors, the combination

TABLE I. Yield per particle event of 1.37-MeV γ rays, I_γ , measured along the scattering normal with a 3-in. \times 3-in. NaI crystal (photopeak efficiency η) at various distances d , from the target; deduced probabilities P_m for the population of the $^{24}\text{Mg}(2^+)$ $|m|$ substates ($P_1 =$ spin-flip probability). The quoted values and errors are obtained from a least-squares fit. Possible systematic errors are discussed in the text.

| $\theta_{c.m.}$ | d (cm) | η (%) | $10^3 I_\gamma$ | P_1 (%) | P_0 (%) | P_2 (%) |
|-----------------|-------------|---------------|-------------------|-----------------|---------------|--------------|
| 10° | 4.6 | 1.41 | 4.90 ± 0.26 | 1.67 ± 0.52 | 4.2 ± 5.5 | 94 ± 5 |
| | 7.5 | 0.75 | 1.45 ± 0.14 | | | |
| | 14.6 | 0.27 | 0.262 ± 0.024 | | | |
| 21° | 4.6 | 1.41 | 2.7 ± 1.5 | 0.50 ± 0.73 | -11 ± 21 | 111 ± 20 |
| | 9.6 | 0.52 | 0.60 ± 0.24 | | | |
| | 24.6 | 0.11 | 0.018 ± 0.016 | | | |

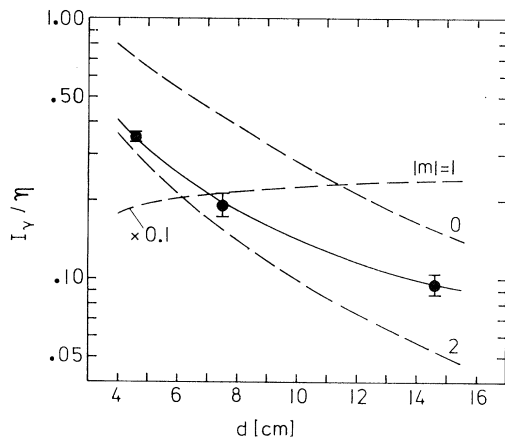


FIG. 2. Out-of-plane intensity of $^{24}\text{Mg}(2^+)$ γ rays per particle event following inelastic ^{13}C scattering at $\theta_{c.m.} = 10^\circ$, divided by the efficiency of the NaI detector for isotropic radiation. The dashed curves show the calculated values of I_γ/η for pure m -substate population of $^{24}\text{Mg}(2^+)$. A fit to the data yields the full curve corresponding to the probabilities of the $|m|$ components given in Table I.

of distances chosen here makes our experiment very sensitive to the $|m|=1$ component but much less so to the $m=0$ component. For example, in Fig. 1 about 40% of the photopeak yield is due to $|m|=1$, although it constitutes only 1.7% of the cross section.

Systematic errors are a concern because they could produce apparent spin flip. Misalignment of the apparatus could allow a tilt of the scattering normal relative to the quantization axis of up to 2.5° . For $P_1=0$, $P_0=10\%$, and $P_2=90\%$ a rotation of the quantization axis yields a maximum apparent P_1' of 0.3% with the most pessimistic assumptions about the unmeasured phases. This is considerably less than the measured value at $\theta_{c.m.}=10^\circ$. By a similar argument the effect of the finite solid angle used for particle detection and of the relativistic transformation due to the recoil velocity may be neglected. A 5% error of the efficiency for γ -ray detection at all distances has a negligible effect. A change of η (4.6 cm) by $\pm 5\%$ with respect to the efficiency at the other distances causes deviations of $\pm 0.2\%$ for P_1 and $\pm 4\%$ for P_0 and P_2 in the $\theta_{c.m.}=10^\circ$ measurements and negligible deviations in the $\theta_{c.m.}=21^\circ$ measurements. Another possible systematic error which might produce excess γ rays along the scattering normal is the effect of hyperfine interactions upon the substate population of the $^{24}\text{Mg } 2^+$ state. This effect is negligible for

two reasons. First, most of the recoiling Mg ions do not leave the target environment, and second, for those that do, a very small effect is produced even for a field of 4 MG acting over the lifetime of 2 psec.

In an optical-model description of the inelastic scattering process, the observed spin flip is commonly attributed to a spin-orbit potential. To determine the spin-independent optical potential we have separately measured the differential cross section for the elastic and inelastic scattering of ^{13}C by ^{24}Mg between $\theta_{c.m.}=7.5^\circ$ and 50° . If the relatively small effect of spin flip on these cross sections is ignored, a good fit¹² is obtained with a Woods-Saxon nuclear potential in the entrance and exit channels, with parameters $V=-40$ MeV, $W=-19.1$ MeV, $R=1.165(24^{1/3}+13^{1/3})$ fm, $a=0.658$ fm and the standard collective excitation form factor composed of the Coulomb term and the first-order approximation of the quadrupole deformation of the nuclear potential given above. The observed strong $|m|=2$ dominance is reproduced by these calculations. To make possible spin flip a spin-orbit potential

$$V_{ls}(r) = -2(\hbar/m_\pi c)^2 V_{s.o.}(1/r)(df/dr)\vec{l} \cdot \vec{s}$$

has been added to the spin-independent potential, where $f(r) = \{1 + \exp[(r-R)/a]\}^{-1}$. The radius and the diffuseness parameters for the spin-orbit term are the same as those stated above. We have not considered an $\vec{l} \cdot \vec{l}$ term acting on the ^{24}Mg spin (\mathbf{I}) in the exit channel nor a deformed $\vec{l} \cdot \vec{s}$ term in the form factor. To account for the 1.7% spin-flip probability observed at $\theta_{c.m.}=10^\circ$ a strength $V_{s.o.} \cong 0.7$ MeV is required for the specific optical potential above. The upper limit of P_1 measured at $\theta_{c.m.}=21^\circ$ is consistent with this result as are upper limits obtained in earlier spin-flip experiments¹³ with ^{13}C . For a $^{13}\text{C} + ^{24}\text{Mg}$ grazing collision with $l_{\text{graz}} = 15\hbar$ the spin-orbit potential deduced from our experiment amounts to 9% of the real potential at $r = 1.5(24^{1/3} + 13^{1/3})$ fm.

Our deduced value for the spin-orbit potential at the strong absorption radius is about a factor of 4 smaller than the value proposed⁵ to solve the phasing problem¹⁴ of the $^{40}\text{Ca}(^{13}\text{C}, ^{14}\text{N})^{39}\text{K}$ differential cross section. However, it exceeds predictions of folding-model calculations,¹⁻³ also performed for the $^{13}\text{C} + ^{40}\text{Ca}$ system, by an order of magnitude or more. It remains to be seen whether inclusion of exchange processes¹⁵ or a proper wave function¹⁶ instead of the single-par-

ticle model wave function may increase the folding-model value.

This experiment has benefitted from help and advice by K. W. Jones, C. E. Thorn, and A. Z. Schwarzschild. One of us (W.D.) would like to acknowledge gratefully the excellent working conditions and hospitality he experienced during his summer visit in Brookhaven National Laboratory. This research was supported by the U. S. Department of Energy, Division of Basic Energy Sciences, under Contract No. EY-76-C-02-0016.

^(a)Summer visitor, 1978. Permanent address: Sektion Physik, Universität München, D-8046 Garching, West Germany.

^(b)Present address: Institute for Nuclear Study, University of Tokyo, Tanashi, Tokyo 188, Japan.

¹W. J. Thompson, in Proceedings of the Symposium on Heavy-Ion Elastic Scattering, Rochester, New York, 1977, edited by R. M. DeVries (unpublished).

²P. J. Moffa, Phys. Rev. C 16, 1431 (1977).

³F. Petrovich, D. Stanley, L. A. Parks, and P. Nagel,

Phys. Rev. C 17, 1642 (1978).

⁴S. Kubono *et al.*, Phys. Rev. Lett. 38, 817 (1977).

⁵B. F. Bayman, A. Dudek-Ellis, and P. J. Ellis, Nucl. Phys. A301, 141 (1978).

⁶P. Wust *et al.*, Z. Phys. A 291, 151 (1979).

⁷F. H. Schmidt *et al.*, Nucl. Phys. 52, 353 (1964).

⁸W. Weiss *et al.*, Phys. Lett. 61B, 237 (1976).

⁹A. Bohr, Nucl. Phys. 10, 2154 (1959).

¹⁰J. B. Marion and F. C. Young, *Nuclear Reaction Analysis* (North Holland, Amsterdam, 1968).

¹¹M. Giannini, P. R. Oliva, and M. C. Ramorino, Nucl. Instrum. Methods 81, 104 (1970); Monte Carlo program EFFNA1, modified version supplied by W. Trautmann, unpublished.

¹²E. H. Auerbach, computer code A-THREE, Comput. Phys. Commun. 15, 165 (1978); P. D. Kunz, computer code DWUCK, unpublished; D. Pelte and U. Smilansky, computer code CCC, unpublished.

¹³C. Chasman, P. D. Bond, and K. W. Jones, Bull. Am. Phys. Soc. 20, 55 (1975); R. Albrecht *et al.*, Max-Planck-Institut, Heidelberg, Annual Report, 1976 (unpublished).

¹⁴P. D. Bond *et al.*, Phys. Rev. Lett. 36, 300 (1976).

¹⁵W. G. Love, Nucl. Phys. A226, 319 (1974).

¹⁶M. B. Golin and S. Kubono, Phys. Rev. C 20, 1347 (1979).

Pre-equilibrium Components of the Fluctuation Cross Section

M. S. Hussein^(a) and K. W. McVoy

Physics Department, University of Wisconsin, Madison, Wisconsin 53706

(Received 20 September 1979)

It is shown that the fluctuation cross section for the generalized-exciton or nested-doorway model can be obtained explicitly and exactly in the limit that doorways of successive classes have very different widths, $\Gamma_n \gg \Gamma_{n+1}$, and that the doorways of a given class are overlapping, $\Gamma_n > D_n$. The result is given in terms of experimentally observable quantities, and explicitly separates the compound and precompound contributions. It contains the results of previous, more specialized, models as limiting cases.

An appealing example of a system whose reactions exhibit precompound components is a model consisting of "nested doorways," such as the exciton model. This model assumes the doorway resonances to be grouped into classes according to their total widths, with $\Gamma_n \equiv \langle \Gamma_{\lambda n} \rangle_\lambda$ the average width in class n . The widths of these doorway classes, assumed to be arranged in the sequence

$$\Gamma_1 \gg \Gamma_2 \gg \dots \gg \Gamma_N, \quad (1)$$

imply a corresponding sequence of time delays $(\Delta t)_n = \hbar/\Gamma_n$, which fix the time scale of the various components of the reaction, from the maximum delay \hbar/Γ_N of the compound-nucleus levels down to \hbar/Γ_1 for the fastest of the precompound

components.

Equation (1) defines a sequence (we might call it a "well-nested" sequence) of classes of compound-nucleus ($n=N$) and doorway ($n < N$) resonances. If we assume that the levels of each class are overlapping,

$$\Gamma_n > D_n, \quad (2)$$

we find that the methods of Kawai, Kerman, and McVoy¹ (KKM), originally employed to obtain the fluctuation cross section in the absence of doorways, can immediately be extended to obtain the exact expression for $\langle \sigma^{f1} \rangle$ in the nested-doorway model as well, without further approximation. The result is obtained with great algebraic sim-